Journal of Electroanalytical Chemistry 703 (2013) 56–62

Contents lists available at SciVerse ScienceDirect

Journal of Electroanalytical Chemistry

journal homepage: www.elsevier.com/locate/jelechem

Glycerol oxidation on nickel based nanocatalysts in alkaline medium – Identification of the reaction products

V.L. Oliveira [a,b], C. Morais [b], K. Servat [b], T.W. Napporn [b], G. Tremiliosi-Filho [a], K.B. Kokoh [b,*]

[a] Instituto de Química de São Carlos, Universidade de São Paulo, C.P. 780, 13560-970 São Carlos, SP, Brazil
[b] Université de Poitiers, IC2MP UMR CNRS 7285, "Equipe SAMCat", 4 rue Michel Brunet, B27, BP 633, 86022 Poitiers cedex, France

ARTICLE INFO

Article history:
Received 23 September 2012
Received in revised form 18 April 2013
Accepted 18 May 2013
Available online 6 June 2013

Keywords:
Glycerol electrooxidation
Nickel
Cobalt
Chromatographic analysis
Spectroscopic measurements

ABSTRACT

In this work, carbon supported nickel based nanoparticles were prepared by impregnation method and used as anode electrocatalysts for the glycerol conversion. These metallic powders were mixed with a suitable amount of a Nafion/water solution to make catalytic inks which were then deposited onto the surface of carbon Toray used as a conductive substrate. Long-term electrolyses of glycerol were carried out in alkaline medium by chronoamperometry experiments. Analysis of the oxidation products was performed with ion-exclusion liquid chromatography which separates the analytes by ascending p*K*a. The spectroscopic measurements have shown that the cobalt content in the anode composition did contribute to the C—C bond cleavage of the initial molecule of glycerol.

1. Introduction

Glycerol is a highly functionalized molecule which results in biosustainable sources such as hydrolysis or methanolysis of triglycerides [1–3]. Among various other applications including this organic compound, glycerol can be used in the production of food additives, pharmaceuticals, personal care products and cosmetics. However, as a co-product obtained during the production of biodiesel, in a short timescale, the large volume of glycerol has exceeded its demand. Therefore, efforts have been made to find new applications to this molecule issued from biomass for fuel and chemicals [3–9]. Many investigations have been conducted on the glycerol oxidation to various compounds. In heterogeneous catalysis the oxidation of glycerol was studied over different types of materials as a function of various reaction parameters such as reaction temperature, oxygen partial pressure, catalyst amount and nature of the catalyst support [1,8,10–14]. Although many reaction products can be obtained from the glycerol oxidation, added value compounds are markedly observed. Dihydroxyacetone which is a self-tanning agent in the cosmetic industry was selectively obtained either on Pt–Bi catalysts [15,16] or Au supported on multi-walled carbon nanotubes at the place of activated carbon [17]. Conversely to heterogeneous catalysis, in electrocatalysis the electrode potential can be controlled to provide or not oxygenated species at the catalyst surface. This implies the possibility of favoring adsorption phenomena at lower potentials on noble metals in the fuel cell applications [18–21]. In this context several investigations were reported on Pt-, Pd- and Au-based anode catalysts under the same conditions than other alcohols (methanol, ethanol and ethylene glycol) [20,22–24]. Glycerol, which is a three-carbon atom compound, is a bit more complex molecule than the alcohols above mentioned with one- and two-carbon atoms. It has a theoretical energy density of 5 kWh kg^{-1} [25], which means that its oxidation can be doubly motivated by providing an alternative and renewable energy source and cogenerating added-value chemicals [19,20]. Nowadays, several studies are being carried out in alkaline medium because of the decrease in poisoning effect on the catalyst in such electrolyte. Hydroxypyruvate, glycerate, mesoxalate, glycolate, tartronate, oxalate and formate ions and dihydroxyacetone are the main reaction products that are observed during the glycerol oxidation reaction [26–28]. CO and CO_2 were also identified by FTIR spectroscopy as other possible reaction products [6,7,29–31]. Under hydrothermal electrolysis conditions, Yuksel et al. have detected particular reaction products such as lactic and acetic acids [32]. As can be seen, various chemicals may be issued from the glycerol oxidation process. The chemical separation of the products formed during the electrooxidation of glycerol is not an elementary task and becomes a real challenge.

The present work is therefore focused on the identification and chromatographic separation of the reaction products when glycerol is anodically converted on noble metal free catalysts in alkaline medium. As stated above, the poisoning effect on the

* Corresponding author. Tel.: +33 5 49 45 4120; fax: +33 5 49 45 3580.
E-mail address: boniface.kokoh@univ-poitiers.fr (K.B. Kokoh).

1572-6657/$ - see front matter © 2013 Elsevier B.V. All rights reserved.
http://dx.doi.org/10.1016/j.jelechem.2013.05.021

catalyst in alkaline medium is low and so, due to its competitive price in comparison with noble and precious metals, nickel becomes a promising and interesting electrode material for the oxidation process of alcohols and polyols [33–35]. Thus, carbon Vulcan XC-72 modified catalysts prepared by nickel and nickel/cobalt impregnation were carefully deposited onto a carbon Toray substrate and used as working electrodes in the glycerol oxidation. Analyses of the oxidation products were performed with ion-exclusion liquid chromatography and FTIR spectroscopy coupled with electrochemical measurements.

2. Experimental

2.1. Synthesis of nickel based electrode nanomaterials

Ni/C and NiCo/C nanomaterials were prepared by a controlled impregnation-reduction method well-described elsewhere [36–38]. Briefly, a suitable amount of carbon Vulcan XC-72 provided by Cabot and $Ni(NO_3)_2{\cdot}6H_2O$ (Aldrich P.A.) were dissolved in ultra pure water (Millipore-MilliQ® water with a resistivity of 18.2 MΩ cm at 20 °C) under sonication for 10 min. The solvent was evaporated in a Petri plate at 80 °C, and the resulting residue was ground to a fine powder before its submission to a thermal treatment. This heat-treatment was conducted in a tubular oven under a H_2 atmosphere at 300 °C with a temperature rate of 5 °C min^{-1}. The same procedure was performed for preparing the NiCo/C catalyst with the addition of $CoCl_2{\cdot}6H_2O$ (Alfa Aesar P.A.) in the solution to reach a nominal atomic ratio Ni/Co of 1:1. The cobalt content in the catalyst requires a heat-treatment at 700 °C for 2 h, which enables the homogenization of the material composition. The Vulcan carbon used as a supporting material has a specific area of 250 $m^2\ g^{-1}$. It was co-impregnated with the catalysts precursors to avoid agglomeration of the particles and it was also obtained with a metal loading of 20 wt.% for each catalyst sample.

2.2. Electrochemical characterization of the catalysts and long-term electrolysis of glycerol

All the electrochemical experiments (cyclic voltammetry and chronoamperometry) were carried out in a Pyrex two-compartment cell. The compartments were separated with an anion-exchange membrane (35 μm thickness, from Fumatech) and were deaerated by ultrapure N_2 (U Quality, from l'Air Liquide). A Reversible Hydrogen Electrode (RHE) and slab of vitreous carbon were used as reference and counter electrode, respectively. The reference electrode was separated from the solution by a Luggin-Haber capillary tip. Among other benefits, the capillary tip avoids the contamination of the RHE gas (H_2) by O_2 which may be formed during electrolysis at high potentials.

The working electrode consisted of catalytic powders deposited on a Carbon Toray used as conductive carrier with a geometric surface area of 3 cm^2. The electrical connection of the carbon Toray substrate was established with a gold wire thanks to a carbon paste. A catalytic ink was prepared from the metal/C powder (2 mg) added in a mixture of 425 μL of Nafion® solution (Aldrich) and 75 μL of water. 50 μL of the catalytic ink was finally deposited onto each face of the carbon Toray sheet and the solvent was evaporated at room temperature; this amount represents 133 μg cm^{-2} of metal loading.

All the electrochemical measurements were carried out using a computer controlled Autolab Potentiostat (PGSTAT 302 N) connected to an Electrochemical Interface (Metrohm). The homemade Ni/C and NiCo/C electrocatalysts were characterized by cyclic voltammetry (CV) in 0.1 mol L^{-1} NaOH (Sigma-Aldrich 97%) as supporting electrolyte. The long-term electrolyses of glycerol (Sigma-Aldrich ⩽99%) was conducted by chronoamperometry (CA) and was performed in potential domains where CV curves showed the formation of metal oxy-hydroxides at the electrode surface.

During the electrochemical experiments, a nitrogen stream was maintained over the electrolytic solutions to prevent their contamination from external carbon dioxide.

2.3. High Performance Liquid Chromatography (HPLC) measurements

The separation and the analysis of the products issued from the glycerol oxidation were performed at 25 °C using a High Performance Liquid Chromatography (HPLC) with the Dionex system (P680 HPLC). It works with an isocratic elution and mainly includes a sample loop (20 μL) previously to the ion-exclusion column (Aminex HPX-87H), which separates the sample compounds by ascending p*K*a (Table 1). When the p*K*a values of compounds are close an additional steric effect can be singled out.

The chromatograph was equipped with an UV–Vis detector followed by a refractive index detector (IOTA2). The column operated at room temperature and the analytes were separated with diluted sulfuric acid (3.3 m mol L^{-1} H_2SO_4) used as eluent. The chromatography system configuration and the operation conditions were critical for effective and successful product separations. The assignments of the different peaks and the quantitative determination of the products were done by comparing the retention times with those of reference samples.

2.4. In situ Fourier transform infrared (FTIR) spectroscopy measurements coupled with electrochemical experiments

In situ FTIR measurements were carried out in a Bruker IFS 66v spectrometer which was modified for beam reflection on the electrode surface at a 65° incidence angle. In order to avoid all interferences from atmospheric water and CO_2 all the system is maintained under vaccum. The detector was a MCT (HgCdTe) type, cooled by liquid nitrogen. The spectral resolution was of 4 cm^{-1} and the FTIR spectra were recorded in 1000–4000 cm^{-1} MIR region. A homemade three-electrode spectroelectrochemical cell, fitted with an MIR transparent window (CaF_2) at the bottom was used. The potentiostat was the same used in electrochemical experiments. A slab of glassy carbon and Reversible Hydrogen Electrode served as counter and reference electrodes, respectively. The working electrode consisted of 5 μL of catalytic ink deposited onto a 8 mm diameter glassy carbon disk. In order to minimize the absorption of the infrared beam by the solution and to study the absorbed species, the working electrode was pressed against the window and a thin layer of electrolytic solution was obtained. Spectra were acquired according to the SPAIRS (Single Potential Alteration IR Spectroscopy) method, performed in the potential range of 0.6–1.9 V vs. RHE and the electrode reflectivity R_{Ei} was recorded at different potentials E_i, each separated by 0.05 V during the voltammogram at a sweep rate of 1 mV s^{-1}.

Table 1
p*K*a values of the organic compounds separated with an ion-exclusion column.

Sample	Oxalic acid/oxalate	Tartronic acid/tartronate	Glyceric acid/glycerate	Glycolic acid/glycolate	Formic acid/formate
p*K*a at 25 °C	pKa_1: 1.25	pKa_1: 2.42	3.55	3.83	3.77

3. Results and discussion

3.1. Cyclic voltammetric study

3.1.1. Cyclic voltammetry of the Ni/C catalyst in the absence and presence of glycerol

Fig. 1 shows the voltammograms of the Ni/C electrode recorded in alkaline medium. The *j–E* dotted line profile concerns the oxidation/reduction of the Ni/C surface in the supporting electrolyte (0.1 mol L^{-1} NaOH). From it one can observe three potential domains:

(i) a double layer domain of Ni in the range 0.6–0.9 V vs. RHE
(ii) the region between 0.9 and 1.38 V vs. RHE, where the surface of the electrode is mainly covered by nickel hydroxides, according to the following equation:

$$Ni + 2HO^- = Ni(OH)_2 + 2e^- \quad (1)$$

(iii) and the region from 1.38 to 1.6 V vs. RHE, which concerns the redox couple Ni(II)/Ni(III), as follows:

$$Ni(OH)_2 + HO^- = NiOOH + H_2O + e^- \quad (2)$$

During the positive going scan, the nickel hydroxide (β-$Ni(OH)_2$) is therefore oxidized to oxy-hydroxide (NiOOH) at *ca.* 1.4 V, while this latter species is reduced at 1.3 V vs. RHE during the negative going scan [39].

When the electrolyte contains 0.1 mol L^{-1} of glycerol the oxidation of the latter molecule starts at *ca.* 1.2 V vs. RHE, i.e. 200 mV under the potential where NiOOH is formed. One should expect that the glycerol oxidation superimposes with the NiOOH surface formation [40–43]. According to other results reported in the literature, alcohol and other organics oxidation begins earlier on the Ni electrode surface. For example, the oxidation of glycerol on hcp-nano Ni modified composite graphite exhibited a 40 mV potential shift [43]. This effect could be associated to the dependency of the beginning of the glycerol oxidation with the preliminary steps of the transformation of $Ni(OH)_2$ to NiOOH. The voltammogram for the glycerol oxidation was recorded with an upper potential limit fixed at 1.9 V vs. RHE, in order to show a more panoramic view of the electrochemical behavior of the reactive species. It can be observed that the glycerol oxidation transforms the original anodic peak of the NiOOH formation into a smooth peak, and the cathodic peak originally observed during the negative going- scan disappears completely.

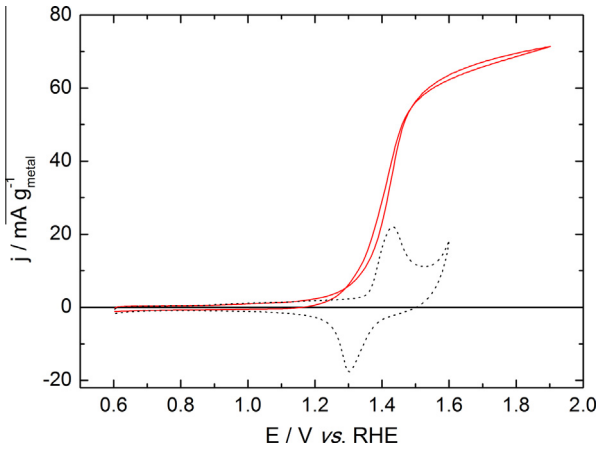

Fig. 1. Voltammograms of a Ni/C electrode recorded at 50 mV s^{-1} in 0.1 mol L^{-1} NaOH without (dotted line) and in the presence of 0.1 mol L^{-1} glycerol (solid line).

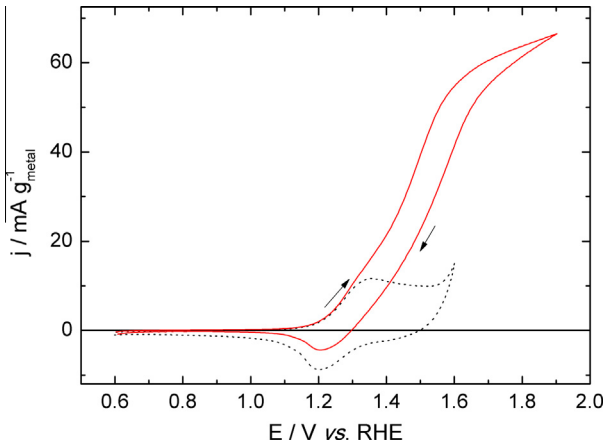

Fig. 2. Voltammograms of a NiCo/C electrode recorded at 50 mV s^{-1} in 0.1 mol L^{-1} NaOH without (dotted line) and in the presence of 0.1 mol L^{-1} glycerol (solid line).

3.1.2. Cyclic voltammetry of the NiCo/C catalyst in the absence and presence of glycerol

Fig. 2 shows the voltammograms of the NiCo/C catalyst in alkaline solution. As can be seen from the corresponding curve obtained in the supporting electrolyte (dotted line), the voltammogram exhibits a similar shape of that of Ni/C (Fig. 1). Nevertheless, some differences appear specially in the potential region of the redox couple $Ni(OH)_2$/NiOOH. The cobalt content in the catalyst composition modifies both, the peak current and the peak potential. The corresponding oxidation peak shows a peak current diminution of *ca.* 45%, and the oxidation peak is less sharp and more spread with a peak potential of 1.35 V vs. RHE. This change in the j–E profile is likely due to the formation of CoOOH from the corresponding cobalt hydroxide, $Co(OH)_2$, that occurs earlier than that of NiOOH [44–48]. According to the results of Gerken et al. [49], the oxidation of dissolved Co^{2+} ions to the insoluble oxy-hydroxide species can be written as:

$$Co^{2+}(aq) + 2H_2O = CoOOH + 3H^+ + e^- \quad (3)$$

with E (V vs. NHE) = 1.747−0.059 log[Co^{2+}]−0.177 pH at 298 K

This identified the formation of CoOOH species on the electrode surface. At higher potentials, the oxide/hydroxide of cobalt can be converted to Co_3O_4 species, as reported by Asgari et al. [45].

As can be noticed in Fig. 2, the glycerol oxidation starts concomitantly with the formation of the CoOOH/NiOOH peak, which

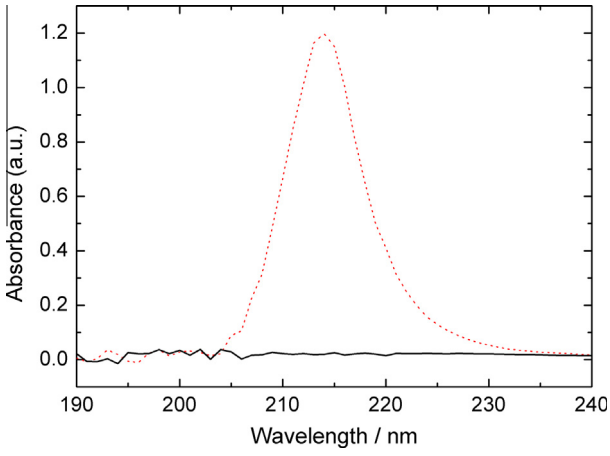

Fig. 3. UV–Vis spectra of the glycerol solution prepared in ultrapure water (solid line) and in 0.1 mol L^{-1} NaOH (dotted line).

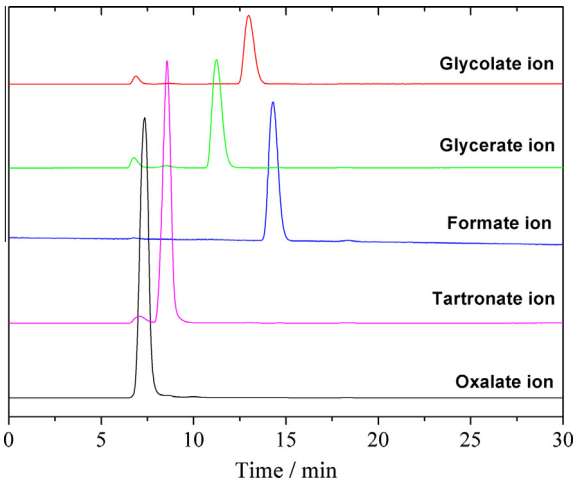

Fig. 4. Chromatographic separation of the reaction products issued from the glycerol oxidation reaction on the Ni/C electrode in a 0.1 mol L^{-1} NaOH solution.

shows their capability of oxidizing alcohols and polyols [33,44,45]. In the presence of glycerol the CV was recorded with an upper potential limit at 1.9 V vs. RHE in anticipation of the next step, the electrolysis or chronoamperometric measurements. As previously stated for Ni electrode, the glycerol oxidation starts at 1.2 V (Fig. 1) while on NiOOH/CoOOH the onset potential for glycerol oxidation is *ca.* 1.1 V (Fig. 2), concomitantly with the formation of both oxy-hydroxides at the surface of the electrode material (Fig. 2), which implies that the catalyst is a mixture of CoOOH and NiOOH.

3.2. Chromatographic analysis of the glycerol oxidation products

Long-term electrolyses of glycerol were carried out at two set potentials, 1.6 V and 1.9 V vs. RHE, during a period of 8 h. Samples of 50 μL of the bulk solution were taken as a function of the time, in order to analyze the products formed during the course of the electrolyses. For this a HPLC device equipped with a 20 μL sample loop was employed. It was noticed, by chromatographic analysis, that the initial solution, before applying any potential and after the deaeration with an inert gas (N_2), presented traces of glycerate. It was then necessary to elucidate the cause of the presence of this carboxylic ion in alkaline solution containing glycerol provided by Sigma-Aldrich. For this reason, the UV–Vis spectra of two samples (glycerol + ultrapure water and glycerol + 0.1 mol L^{-1} NaOH) were recorded on a UV–Vis spectrophotometer (Helios Omega UV–Vis from Thermo Scientific) (Fig. 3). As can be seen, a band centered at 215 nm, characteristic of C=O, appears in the sample prepared in alkaline medium. This band confirms the presence of glycerate resulting from HO^- nucleophile attack of glyceraldehyde, an impurity contained into glycerol. From now on, glycerate in the

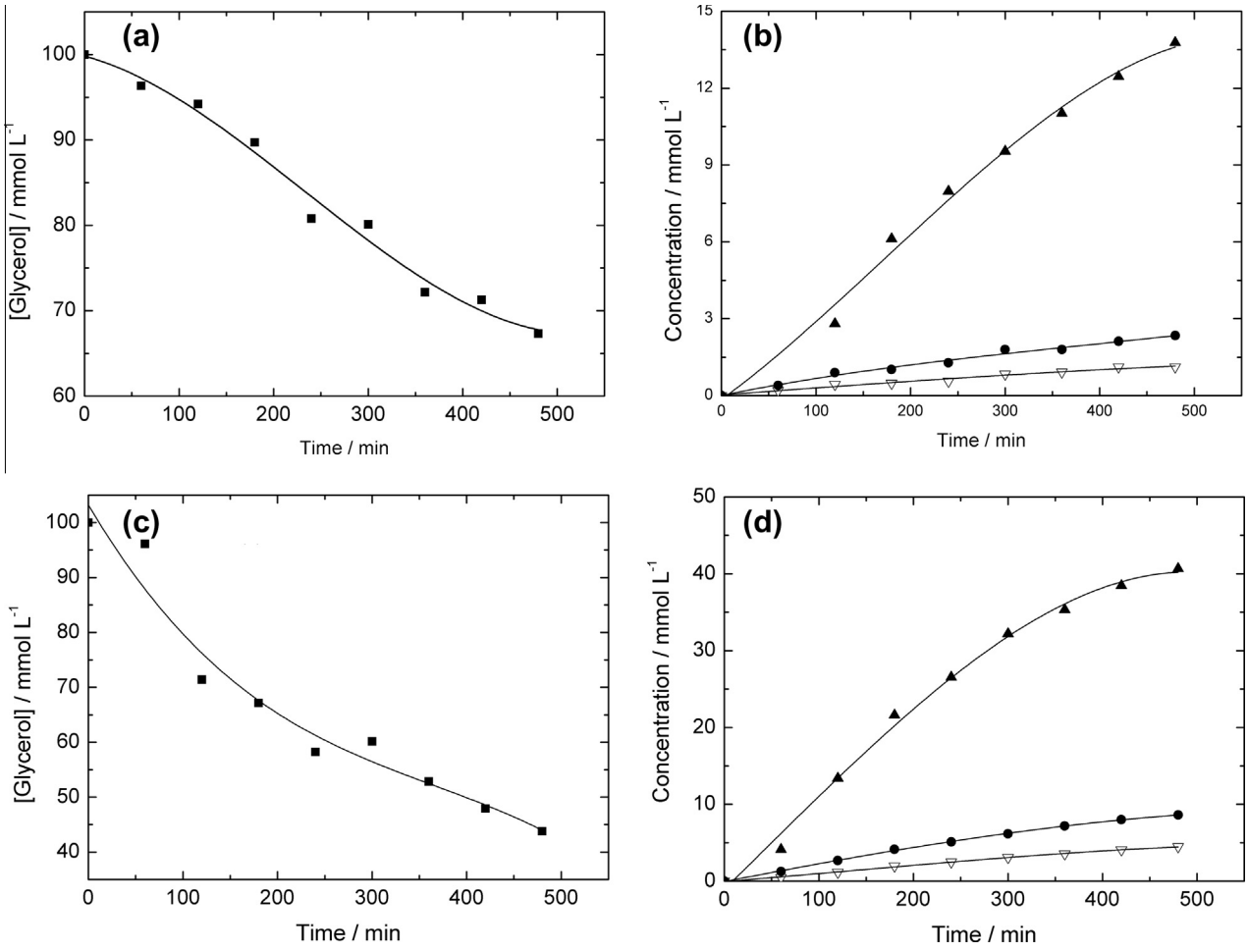

Fig. 5. Plots giving the concentration of reaction product vs. time during the glycerol electrooxidation on Ni/C in 0.1 mol L^{-1} NaOH. At 1.6 V vs. RHE: (a) (■) glycerol conversion; (b) reaction products: (▽) glycerate, (●) glycolate, (▲) formate. At 1.9 V vs. RHE: (c) (■) glycerol conversion; (d) reaction products: (▽) glycerate, (●) glycolate, (▲) formate.

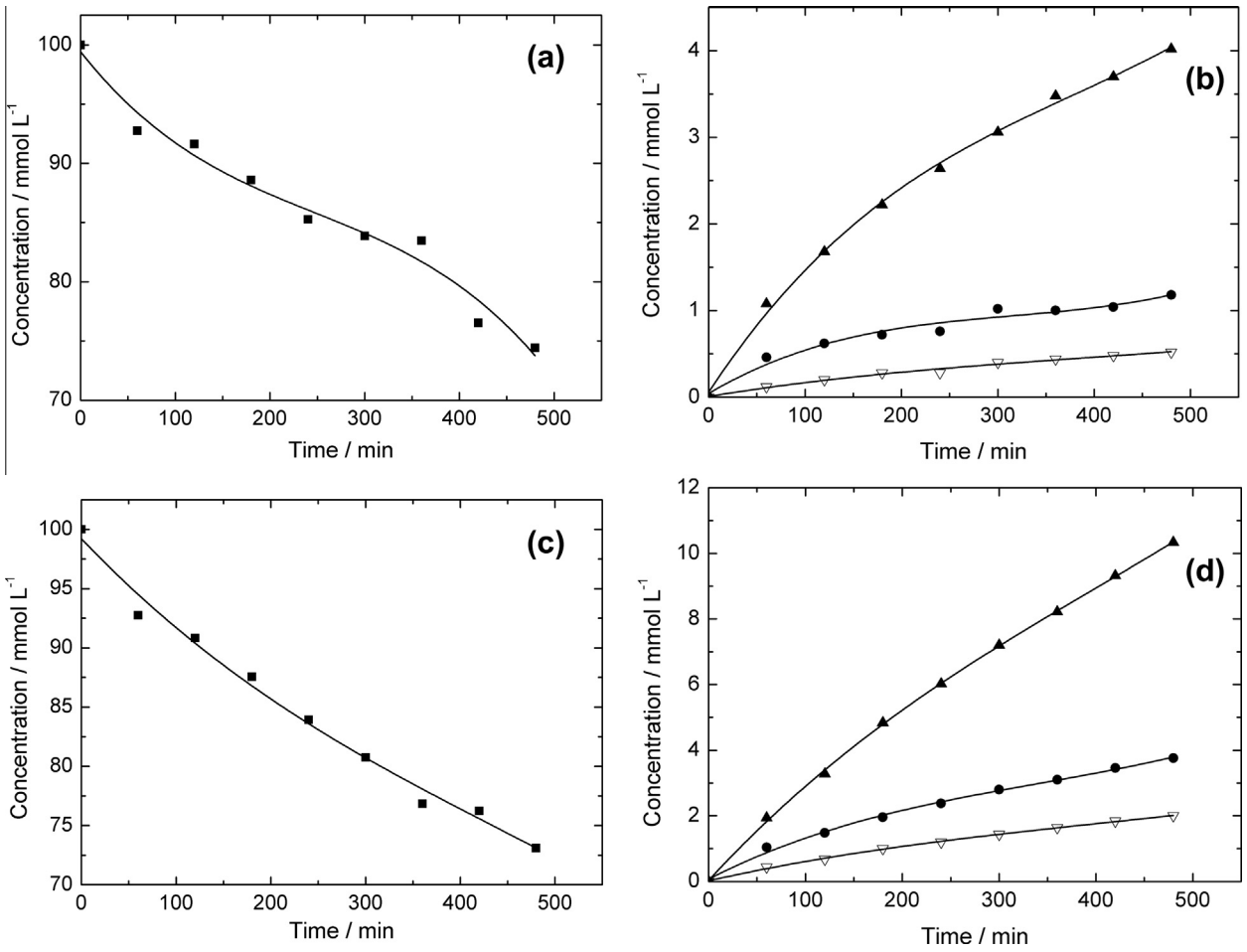

Fig. 6. Plots giving the concentration of reaction product vs. time during the glycerol electrooxidation on NiCo/C in 0.1 mol L^{-1} NaOH. At 1.6 V vs. RHE: (a) (■) glycerol conversion; (b) reaction products: (▽) glycerate, (●) glycolate, (▲) formate. At 1.9 V vs. RHE: (c) (■) glycerol conversion; (d) reaction products: (▽) glycerate, (●) glycolate, (▲) formate.

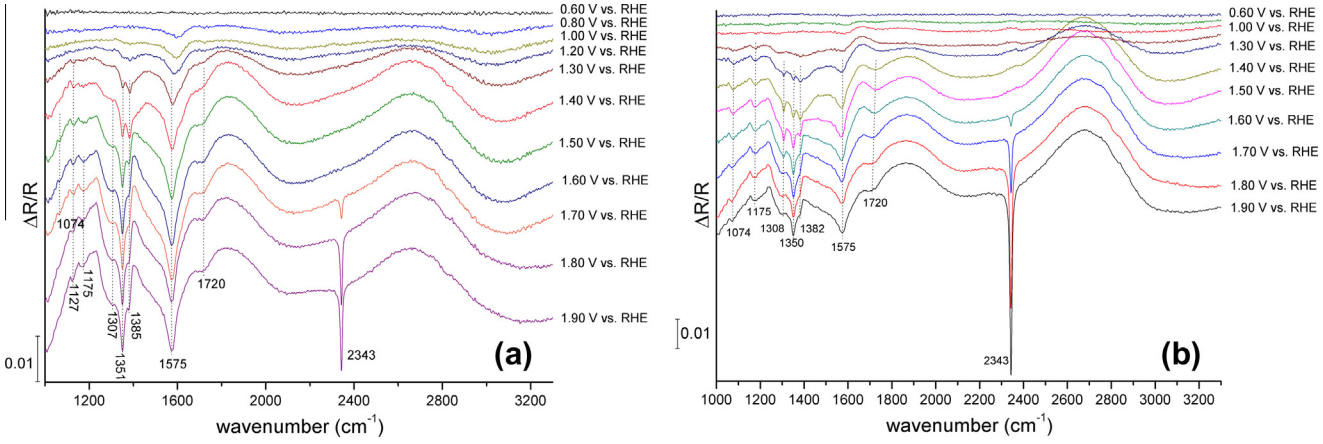

Fig. 7. SPAIR spectra of 0.1 mol L^{-1} glycerol in 0.1 mol L^{-1} NaOH on (a) Ni/C and (b) NiCo/C electrodes at different potentials varying from 0.6 V to 1.9 V vs. RHE and at 1 mV s^{-1}. Reference R_{Ei} was taken at 0.6 V vs. RHE.

electrolytic samples will be therefore quantified by taking the initial chromatogram as background.

3.2.1. Glycerol oxidation on Ni/C

Long-term electrolyses of 0.1 mol L^{-1} glycerol solutions were carried out in alkaline medium at 1.6 and 1.9 V vs. RHE, respectively, at the Ni/C electrode. After successful separation of the analytes, it was possible to follow the variation of the concentration of the reactant and products. Fig. 4 shows the chromatograms of the product formed after the electrolyses at 1.6 and 1.9 V vs. RHE.

Regarding Fig. 1, the current densities are higher at 1.9 V vs. RHE than those involved at 1.6 V vs. RHE. This is predictable because the current intensity is proportional to the reaction rate at the same electrode surface:

$$I = \frac{dQ}{dt} = -nF\frac{dN}{dt} = nFv \quad (4)$$

where dQ is the quantity of electricity involved in the oxidation of a given amount of glycerol during the period dt; n is the number of electrons exchanged, F the Faraday constant, dN, the number of mole of glycerol consumed during the period dt, and v the reaction velocity.

Therefore, and apart from the higher conversion rate of glycerol at 1.9 V vs. RHE, the products distribution is similar at the two oxidation potentials (Fig. 5). Glycerate, glycolate and formate are the main reaction products obtained during the glycerol oxidation at the Ni/C surface in alkaline medium. Small amounts of oxalate and tartronate were also identified.

3.2.2. Glycerol oxidation on NiCo/C

Similar electrolytic processes at the same potentials were carried out at the NiCo/C anode material. As can be observed in Fig. 6, the introduction of the Co content in the material composition modifies the products distribution during the glycerol oxidation in alkaline medium. The formate ion remains the main reaction product, which means that the cobalt oxy-hydroxides do contribute to the cleavage of the C—C bond of the mother molecule. Bubbles of O_2 were observed at the NiCo/C electrode during the glycerol oxidation. As CoOOH is formed earlier than NiOOH, parallel reactions such as CoO_2 from CoOOH oxidation and O_2 production from water decomposition can be Faradaic contributions at $E > 1.6$ V vs. RHE [47].

In the oxidation of primary alcohols at the nickel and cobalt electrodes in alkaline solution, Fleischmann et al. [33,34,44] proposed that the organic species react, as follows:

$$Ni(OH)_2 + HO^- \rightarrow NiOOH + H_2O + e^- \quad (5)$$

$$NiOOH + RCH_2OH + HO^- \rightarrow Ni(OH)_2 + H_2O + e^- + RCHO \quad (6)$$

$$RCHO + 3HO^- \rightarrow RCOO^- + 2H_2O + 2e^- \quad (7)$$

As mentioned in Eq. (6), the reaction mechanism seems to include a glycerol transformation through the formation of glyceraldehyde. Conversely to the literature [26–28] glyceraldehyde was not herein detected as electrooxidation product. This suggests that either this step is so fast that the aldehyde could not be determined chromatographically in the bulk solution, or the HO^- nucleophiles are very efficient to oxidize it to glycerate before its desorption and diffusion to the bulk solution.

3.3. In situ FTIR spectroelectrochemical experiments

To gain further insights into how glycerol is electrooxidized in alkaline medium on these nanoscale materials, *in situ* spectroelectrochemical experiments have been undertaken. Fig. 7 displays the single potential alteration infrared spectra (SPAIRS) obtained for Ni/C and NiCo/C catalysts during glycerol oxidation in alkaline medium. It should be noticed that positive going bands are attributed to glycerol and OH^- consumption while negative going bands correspond to the different products or intermediates formed during glycerol oxidation. Several bands corresponding to different products have been identified: formate ion (1351, 1389 and 1575 cm^{-1}), glycerate ion (1308 cm^{-1}) and glycolate ion (1076 cm^{-1}). The presence of small amounts of oxalate, tartronate and mesoxalate ions cannot be excluded since the band at 1575 cm^{-1} is also characteristic of these species. The broad band at 1720 cm^{-1} is characteristic of the C═O stretching vibration of a C—COO^-. The bands located at 1175 and 1127 cm^{-1} may be attributed to CH_2 bending vibrations confirming therefore the presence of glycolate and/or glycerate ions. These results are in good agreement with the HPLC analysis bringing to light additionally the presence of the hydroxypyruvate ion. Another important result is the evidence of production of CO_2 at high potential values (asymmetric stretching band at 2343 cm^{-1}). According to Demarconnay et al. [50], CO_2 appears as soon as carbonate (1390–1420 cm^{-1} band) could not be further formed due to the lack of OH^-. Jeffery and Camara [30] have proved that in the thin electrolyte layer between the CaF_2 window and the electrode interface, the depletion of OH^- is enough to explain an important pH change during glycerol electrooxidation in alkaline medium. The acidification of the thin layer between the working electrode and the CaF_2 window is clearly shown and part of the recorded current intensity should therefore be related to CO_2 production which cannot be detected by HPLC. Furthermore, at high potential values we cannot exclude the contribution related to the oxygen evolution reaction (OER) since bubbles are visible at the electrode surface.

4. Conclusions

Free-noble metal Ni/C and NiCo/C nanocatalysts deposited onto a carbon Toray substrate were used as electrodes for glycerol oxidation. It was found that for both materials glycerol oxidation took place at potentials higher than 1.2 V vs. RHE, starting therefore before the Ni and Co oxy-hydroxides formation. The reaction products from long-term electrolysis of glycerol were successfully separated on HPX-87H column. Glycerate, glycolate and formate were the main compounds determined by the performed analytical procedure and small amounts of tartronate and oxalate were also detected. Complementary *in situ* FTIR measurements brought to light the presence of the hydroxypyruvate ion and CO_2 as reaction products. Regarding the larger amount of CO_2 formed when using the NiCo/C nanocatalyst as electrode material, one can state that the cobalt content in the nickel based catalyst enhances the C—C bond cleavage of the glycerol molecule which is certainly due to the presence of CoOOH species earlier formed than those of NiOOH. Conversely to reaction mechanisms proposed in the literature, no aldehyde such as glyceraldehyde was detected in the course of the glycerol oxidation reaction. Nevertheless, the reactant provided by Sigma-Aldrich and used as received contains traces of glyceraldehyde chemically transformed into glycerate by HO^- nucleophilic species of the supporting electrolyte.

Acknowledgements

This work was mainly conducted within the framework of a collaborative programme CAPES/COFECUB under Grant No Ch 747-12. V.L. Oliveira also thanks the CAPES Foundation (Grant No 5444110) for providing a travelling scholarship and FAPESP (Grant No 2008/11601-7).

References

[1] S. Carrettin, P. McMorn, P. Johnston, K. Griffin, C.J. Kiely, G.A. Attard, G.J. Hutchings, Oxidation of glycerol using supported gold catalysts, Top. Catal. 27 (2004) 131–136.
[2] A. Wolfson, C. Dlugy, Glycerol as an alternative green medium for carbonyl compound reductions, Org. Commun. 2 (2009) 34–41.
[3] B. Katryniok, H. Kimura, E. Skrzynska, J.-S. Giradon, P. Fongarland, M. Capron, R. Ducoulombier, N. Mimura, S. Paul, F. Dumeignil, Selective catalytic oxidation of glycerol: Perspectives for high value chemicals, Green Chem. 13 (2011) 1960–1979.
[4] A. Marinas, R.A. Sheldon, Utilisation of biomass for fuels and chemicals: the road to sustainability, Catal. Today 167 (2011) 1–2.
[5] M. Lo Faro, M. Minutoli, G. Monforte, V. Antonucci, A.S. Aricò, Glycerol oxidation in solid oxide fuel cells based on a Ni-perovskite electrocatalyst, Biomass Bioenergy 35 (2011) 1075–1084.
[6] J.F. Gomes, F.B.C. de Paula, L.H.S. Gasparotto, G. Tremiliosi-Filho, The influence of the Pt crystalline surface orientation on the glycerol electro-oxidation in acidic media, Electrochim. Acta 76 (2012) 88–93.

[7] J. Gomes, G. Tremiliosi-Filho, Spectroscopic studies of the glycerol electro-oxidation on polycrystalline au and pt surfaces in acidic and alkaline media, Electrocatalysis 2 (2011) 96–105.
[8] S. Carrettin, P. McMorn, P. Johnston, K. Griffin, C.J. Kiely, G.J. Hutchings, Oxidation of glycerol using supported Pt, Pd and Au Catalysts, PCCP 5 (2003) 1329–1336.
[9] G.P. da Silva, M. Mack, J. Contiero, Glycerol: A promising and abundant carbon source for industrial microbiology, Biotechnol. Adv. 27 (2009) 30–39.
[10] F. Porta, L. Prati, Selective oxidation of glycerol to sodium glycerate with gold-on-carbon catalyst: an insight into reaction selectivity, J. Catal. 224 (2004) 397–403.
[11] N. Dimitratos, C. Messi, F. Porta, L. Prati, A. Villa, Investigation on the behaviour of Pt(0)/carbon and Pt(0), Au(0)/carbon catalysts employed in the oxidation of glycerol with molecular oxygen in water, J. Mol. Catal. A: Chem. 256 (2006) 21–28.
[12] A. Villa, A. Gaiassi, I. Rossetti, C.L. Bianchi, K. van Benthem, G.M. Veith, L. Prati, Au on $MgAl_2O_4$ spinels: the effect of support surface properties in glycerol oxidation, J. Catal. 275 (2010) 108–116.
[13] L. Prati, M. Rossi, Gold on carbon as a new catalyst for selective liquid phase oxidation of diols, J. Catal. 176 (1998) 552–560.
[14] E.G. Rodrigues, M.F.R. Pereira, J.J.M. Órfão, Glycerol oxidation with gold supported on carbon xerogels: tuning selectivities by varying mesopore sizes, Appl. Catal. B: Environ. 115–116 (2012) 1–6.
[15] H. Kimura, Selective oxidation of glycerol on a platinum–bismuth catalyst by using a fixed bed reactor, Appl. Catal. A: General 105 (1993) 147–158.
[16] W. Hu, D. Knight, B. Lowry, A. Varma, Selective oxidation of glycerol to dihydroxyacetone over Pt−Bi/C catalyst: optimization of catalyst and reaction conditions, Ind. Eng. Chem. Res. 49 (2010) 10876–10882.
[17] E.G. Rodrigues, M.F.R. Pereira, J.J. Delgado, X. Chen, J.J.M. Órfão, Enhancement of the selectivity to dihydroxyacetone in glycerol oxidation using gold nanoparticles supported on carbon nanotubes, Catal. Commun. 16 (2011) 64–69.
[18] K. Matsuoka, Y. Iriyama, T. Abe, M. Matsuoka, Z. Ogumi, Alkaline direct alcohol fuel cells using an anion exchange membrane, J. Power Sources 150 (2005) 27–31.
[19] Z. Zhang, L. Xin, W. Li, Electrocatalytic oxidation of glycerol on Pt/C in anion-exchange membrane fuel cell: cogeneration of electricity and valuable chemicals, Appl. Catal. B: Environ. 119–120 (2012) 40–48.
[20] M. Mougenot, A. Caillard, M. Simoes, S. Baranton, C. Coutanceau, P. Brault, PdAu/C catalysts prepared by plasma sputtering for the electro-oxidation of glycerol, Appl. Catal. B: Environ. 107 (2011) 372–379.
[21] A. Ilie, M. Simoes, S. Baranton, C. Coutanceau, S. Martemianov, Influence of operational parameters and of catalytic materials on electrical performance of direct glycerol solid alkaline membrane fuel cells, J. Power Sources 196 (2011) 4965–4971.
[22] L. Demarconnay, C. Coutanceau, J.M. Léger, Study of the oxygen electroreduction at nanostructured PtBi catalysts in alkaline medium, Electrochim. Acta 53 (2008) 3232–3241.
[23] C. Coutanceau, L. Demarconnay, C. Lamy, J.M. Léger, Development of electrocatalysts for solid alkaline fuel cell (SAFC), J. Power Sources 156 (2006) 14–19.
[24] V. Bambagioni, C. Bianchini, A. Marchionni, J. Filippi, F. Vizza, J. Teddy, P. Serp, M. Zhiani, Pd and Pt–Ru anode electrocatalysts supported on multi-walled carbon nanotubes and their use in passive and active direct alcohol fuel cells with an anion-exchange membrane (alcohol = methanol, ethanol, glycerol), J. Power Sources 190 (2009) 241–251.
[25] C. Lamy, J.-M. Léger, Les piles à combustible: application au véhicule électrique, J. Phys. IV Fr. 04 (1994). C1-253–C1-281.
[26] Y. Kwon, Y. Birdja, I. Spanos, P. Rodriguez, M.T.M. Koper, Highly selective electro-oxidation of glycerol to dihydroxyacetone on platinum in the presence of bismuth, ACS Catal. 2 (2012) 759–764.
[27] Y. Kwon, K.J.P. Schouten, M.T.M. Koper, Mechanism of the catalytic oxidation of glycerol on polycrystalline gold and platinum electrodes, ChemCatChem 3 (2011) 1176–1185.
[28] Y. Kwon, M.T.M. Koper, Combining voltammetry with HPLC: application to electro-oxidation of glycerol, Anal. Chem. 82 (2010) 5420–5424.
[29] P.S. Fernández, M.E. Martins, G.A. Camara, New insights about the electro-oxidation of glycerol on platinum nanoparticles supported on multi-walled carbon nanotubes, Electrochim. Acta 66 (2012) 180–187.
[30] D.Z. Jeffery, G.A. Camara, The formation of carbon dioxide during glycerol electrooxidation in alkaline media: first spectroscopic evidences, Electrochem. Commun. 12 (2010) 1129–1132.
[31] M. Simões, S. Baranton, C. Coutanceau, Electro-oxidation of glycerol at Pd based nano-catalysts for an application in alkaline fuel cells for chemicals and energy cogeneration, Appl. Catal. B: Environ. 93 (2010) 354–362.
[32] A. Yuksel, H. Koga, M. Sasaki, M. Goto, Hydrothermal electrolysis of glycerol using a continuous flow reactor, Ind. Eng. Chem. Res. 49 (2010) 1520–1525.
[33] M. Fleischmann, K. Korinek, D. Pletcher, The kinetics and mechanism of the oxidation of amines and alcohols at oxide-covered nickel, silver, copper, and cobalt electrodes, J. Chem. Soc., Perkin Trans. 2 (1972) 1396–1403.
[34] M. Fleischmann, K. Korinek, D. Pletcher, The oxidation of organic compounds at a nickel anode in alkaline solution, J. Electroanal. Chem. Interfacial Electrochem. 31 (1971) 39–49.
[35] E. Verlato, S. Cattarin, N. Comisso, A. Gambirasi, M. Musiani, L. Vázquez-Gómez, Preparation of Pd-modified Ni foam electrodes and Their use as anodes for the oxidation of alcohols in basic media, Electrocatal 3 (2012) 48–58.
[36] F.H.B. Lima, D. Profeti, W.H. Lizcano-Valbuena, E.A. Ticianelli, E.R. Gonzalez, Carbon-dispersed Pt–Rh nanoparticles for ethanol electro-oxidation. Effect of the crystallite size and of temperature, J. Electroanal. Chem. 617 (2008) 121–129.
[37] J. Zhang, F.H.B. Lima, M.H. Shao, K. Sasaki, J.X. Wang, J. Hanson, R.R. Adzic, Platinum monolayer on nonnoble metal-noble metal core–shell nanoparticle electrocatalysts for O_2 reduction, J. Phys. Chem. B 109 (2005) 22701–22704.
[38] G.A. Camara, R.B. de Lima, T. Iwasita, The influence of PtRu atomic composition on the yields of ethanol oxidation: a study by in situ FTIR spectroscopy, J. Electroanal. Chem. 585 (2005) 128–131.
[39] A. Visintin, W.E. Triaca, A.J. Arvia, A phenomenological approach to hydrous nickel oxide electrodes prepared by applying periodic potential routines, J. Appl. Electrochem. 26 (1996) 493–502.
[40] Y.L. Chen, T.C. Chou, Paired electrooxidation Part III: Production of n-butyric acid from n-butanol, J. Appl. Electrochem. 26 (1996) 543–545.
[41] S. Majdi, A. Jabbari, H. Heli, A study of the electrocatalytic oxidation of aspirin on a nickel hydroxide-modified nickel electrode, J. Solid State Electrochem. 11 (2007) 601–607.
[42] M. Shamsipur, M. Najafi, M.-R.M. Hosseini, Highly improved electrooxidation of glucose at a nickel(II) oxide/multi-walled carbon nanotube modified glassy carbon electrode, Bioelectrochem. 77 (2010) 120–124.
[43] R.M.A. Tehrani, S. Ab Ghani, Electrocatalysis of free glycerol at a nanonickel modified graphite electrode and its determination in biodiesel, Electrochim. Acta 70 (2012) 153–157.
[44] D. Pletcher, M. Fleischmann, K. Korinek, The oxidation of organic compounds at a cobalt electrode in alkaline media, J. Electroanal. Chem. Interfacial Electrochem. 33 (1971) 478–479.
[45] M. Asgari, M.G. Maragheh, R. Davarkhah, E. Lohrasbi, A.N. Golikand, Electrocatalytic oxidation of methanol on the nickel–cobalt modified glassy carbon electrode in alkaline medium, Electrochim. Acta 59 (2012) 284–289.
[46] X. Li, H. Dong, J. Li, X. Tongchi, Ball milled cobalt oxyhydroxide coat on the surface of nickel hydroxide, J. Appl. Electrochem. 40 (2010) 73–77.
[47] W.E. Triaca, A.J. Arvia, T. Kessler, Electroformation of electrocatalytically active hydrous oxide layers on a Co–Ni amorphous alloy under pulsating electrolysis, J. Appl. Electrochem. 23 (1993) 655–661.
[48] E. Gomez, J. Ramirez, E. Vallés, Electrodeposition of Co–Ni alloys, J. Appl. Electrochem. 28 (1998) 71–79.
[49] J.B. Gerken, J.G. McAlpin, J.Y.C. Chen, M.L. Rigsby, W.H. Casey, R.D. Britt, S.S. Stahl, Electrochemical water oxidation with cobalt-based electrocatalysts from pH 0–14: the thermodynamic basis for catalyst structure, stability, and activity, J. Am. Chem. Soc. 133 (2011) 14431–14442.
[50] L. Demarconnay, S. Brimaud, C. Coutanceau, J.M. Léger, Ethylene glycol electrooxidation in alkaline medium at multi-metallic Pt based catalysts, J. Electroanal. Chem. 601 (2007) 169–180.